



OPEN

SUBJECT AREAS:

PALAEOCLIMATE
PHYSICAL OCEANOGRAPHY

Received

10 December 2013

Accepted

13 February 2014

Published

18 March 2014

Correspondence and
requests for materials
should be addressed to
J.Z. (jens.zinke@uwa.
edu.au)

Madagascar corals track sea surface temperature variability in the Agulhas Current core region over the past 334 years

J. Zinke¹, B. R. Loveday², C. J. C. Reason², W.-C. Dullo³ & D. Kroon⁴

¹The University of Western Australia Oceans Institute, School of Earth and Environment, Australian Institute of Marine Science, Nedlands, WA 6009, Australia, ²Department of Oceanography, University of Cape Town, Rondebosch, 7701, South Africa, ³GEOMAR Helmholtz Centre for Ocean Research Kiel, Wischhofstr. 1-3, 24148 Kiel, Germany, ⁴University of Edinburgh, Grant Institute, The King's Buildings, West Mains Road, Edinburgh EH9 3JW, UK.

The Agulhas Current (AC) is the strongest western boundary current in the Southern Hemisphere and is key for weather and climate patterns, both regionally and globally. Its heat transfer into both the midlatitude South Indian Ocean and South Atlantic is of global significance. A new composite coral record (Ifaty and Tular massive *Porites* corals), is linked to historical AC sea surface temperature (SST) instrumental data, showing robust correlations. The composite coral SST data start in 1660 and comprise 200 years more than the AC instrumental record. Numerical modelling exhibits that this new coral derived SST record is representative for the wider core region of the AC. AC SSTs variabilities show distinct cooling through the Little Ice Age and warming during the late 18th, 19th and 20th century, with significant decadal variability superimposed. Furthermore, the AC SSTs are teleconnected with the broad southern Indian and Atlantic Oceans, showing that the AC system is pivotal for inter-ocean heat exchange south of Africa.

The greater Agulhas Current (AC) system near the southern tip of Africa is a key component in the global climate system through its role in inter-ocean heat and salt transport, thereby influencing the Atlantic meridional overturning circulation^{1–3} (hereafter AMOC). Modeling experiments suggest that the increased export of AC waters into the Atlantic Ocean, through the so-called Agulhas leakage, results in an enhanced AMOC albeit with a lag of 15–30 years^{4–7}. There is mounting evidence that the AC SSTs have increased since the early 1980's⁸. The recent warming is thought to be related to an increase in ocean heat transport in response to an increase in wind stress curl in the southern Indian Ocean trade winds^{8,9}.

The AC is the strongest western boundary current in the Southern Hemisphere and releases a lot of heat to the atmosphere throughout the year. Relatively strong winds over the southern AC lead to strong latent heat loss from the surface, while further north off the east coast of South Africa, there is often convective cloud cover over its warm core^{10–13}. As a result, under suitable atmospheric conditions, the AC can influence severe weather systems over South Africa, Botswana, Zimbabwe and Mozambique such as cut-off lows¹⁴, thunderstorms¹⁵, and mesoscale convective complexes¹⁶.

The AC region is modulated by interannual and decadal climate modes in the Indian and Pacific Ocean, partly through their influence on the circulation in the South Indian Ocean^{17–20} and also through local ocean-atmosphere interactions driven by these modes^{17,21–23}. This strong interannual and decadal variability may be superimposed on the long-term trend in AC SST that could partly be related to changes in the subtropical Indian Ocean gyre strength on these time scales^{24–26}. The Indian Ocean gyres weaken during El Niño or positive Indian Ocean Dipole (hereafter IOD) events whereas they strengthen during La Niña or negative IOD events. The same holds true for subtropical Indian Ocean dipole (hereafter SIOD) phases^{18,20}. On decadal time scales, ENSO-like (El Niño–Southern Oscillation) decadal variability and/or the Pacific Decadal Oscillation (PDO) is thought to exert an influence on southwestern Indian Ocean SST and atmospheric circulation^{22,27}.

Historical gridded SST data and reconstructions reveal that the southern Mozambique Channel (MC), one of the source regions of the AC, has also experienced one of the highest rates in ocean warming across the southern Indian Ocean since 1950²⁸. The instrumental SST reconstructions for the southern MC and the AC core regions

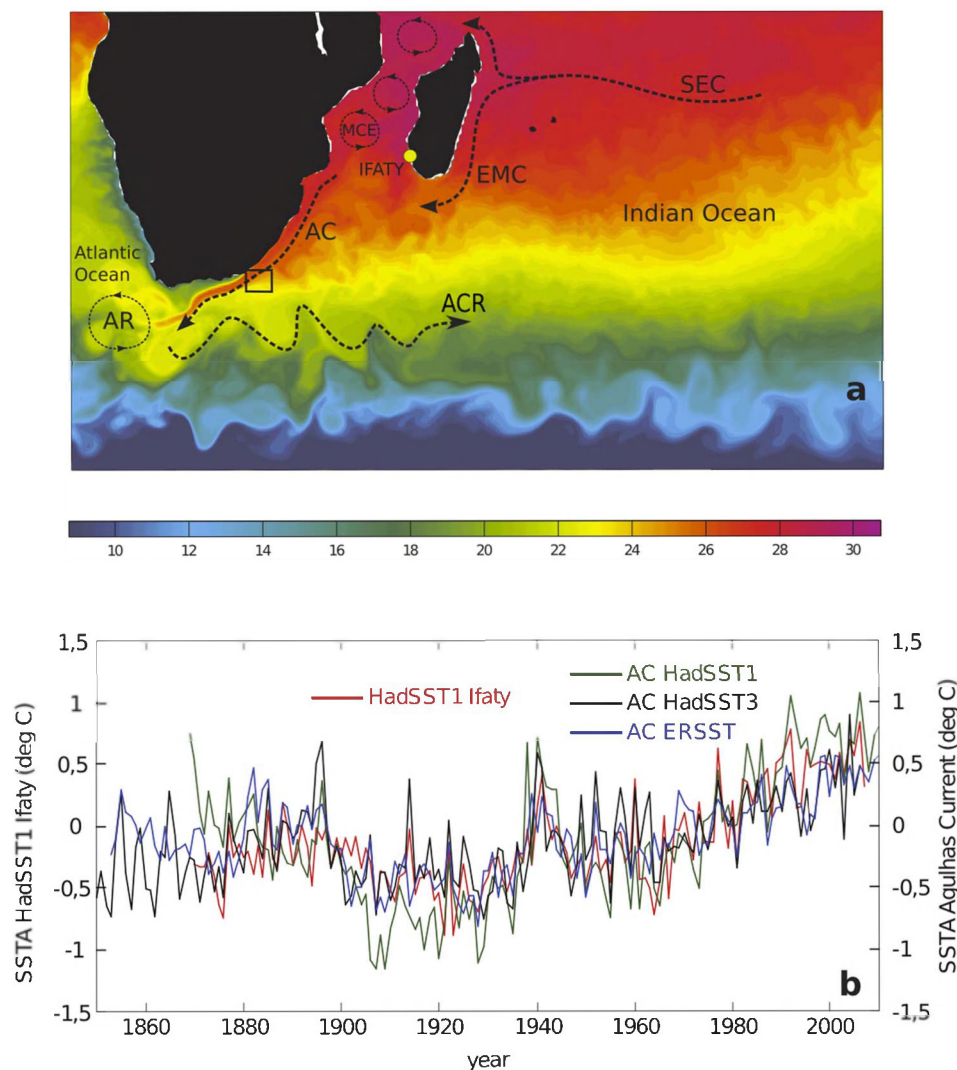


Figure 1 | Surface ocean connectivity between southwest Madagascar and the Agulhas Current. (a) Sea surface temperatures for February 1994 (austral summer) across the southwestern Indian Ocean with the major ocean currents indicated: SEC = South Equatorial Current, EMC = East Madagascar Current, AC = Agulhas Current, ACR = Agulhas Current return flow, MCE = Mozambique Channel Eddies. The Ifaty coral core location (yellow dot) and the region of dense SST observations (rectangular box) for the Agulhas Current are indicated. (b) Sea surface temperature anomalies (SSTA) relative to the 1961 to 1990 period for the grid box closest to the Ifaty/Tulear coral core sites (red) compared to the Agulhas Current core region data from HadSST1³² (green), ERSSTv3b³⁴ (blue) and HadSST3³³ (black). Note the strong co-variability of Ifaty and Agulhas core region SST on multi-decadal time scales. Figure 1a produced at <http://iridl.ldeo.columbia.edu/> and used with permission (data from ref. 44).

show considerable multidecadal variability (Fig. 1). A single 334 year long coral geochemical proxy record from Ifaty reef off southwestern Madagascar in the southern MC also revealed an increase in SST after the 1970's²⁰. This coral record revealed a non-stationary relationship of local southern MC SST with ENSO, and a link with the Pacific Decadal Oscillation²⁷. These single core observations, however, are limited and may not represent the wider southern MC or the AC core region as yet.

The aims of this paper are to produce a new composite coral record to obtain a SST record representing SST changes in the wider southern MC and the AC core regions. Here, we present a new three-core coral composite oxygen isotope record from the Ifaty and Tulear coral reefs off SW Madagascar, which covers SST variability for the past 334 years (1660–1994). Through modeling, we investigated whether the southern MC SST data are representative for the downstream AC core region. Finally, we aim to infer cross-ocean relationships in the Southern Hemisphere using SST records, elucidating the pivotal role of the AC region at the cross roads between the Indian and Atlantic Oceans.

Results

Connectivity between the Ifaty coral site and the Agulhas Current core region, at 32°S. First, we tested connectivity in ocean properties, namely SST and salinity (SSS), between the Ifaty coral site and the Agulhas core region at 32°S, the so-called CAP (Lagrangian virtual floats capture area) area in Figure 2. We use the 5-daily output from a 1948 to 2007 hindcast of a 1/4°, eddy-permitting, basin-scale ocean model²⁹ (Fig. 2). To establish connectivity between the Ifaty site and the downstream AC core region, we correlate the detrended monthly-mean SSS and SST time series from Ifaty with those extracted across the AC source regions and western Indian Ocean boundary (Fig. 2a, b). Our results suggest that SSS and SST across most of the regions of the southern MC and southwestern Indian Ocean boundary are correlated. Further, we find a strong SST and SSS relationship between the Ifaty site and AC core region, shown by the same inter-annual surface variability with zero lag (Fig. 2c).

To assess the time scales of horizontal ocean transport (advection) between the Ifaty site and the AC at 32°S, Lagrangian virtual floats

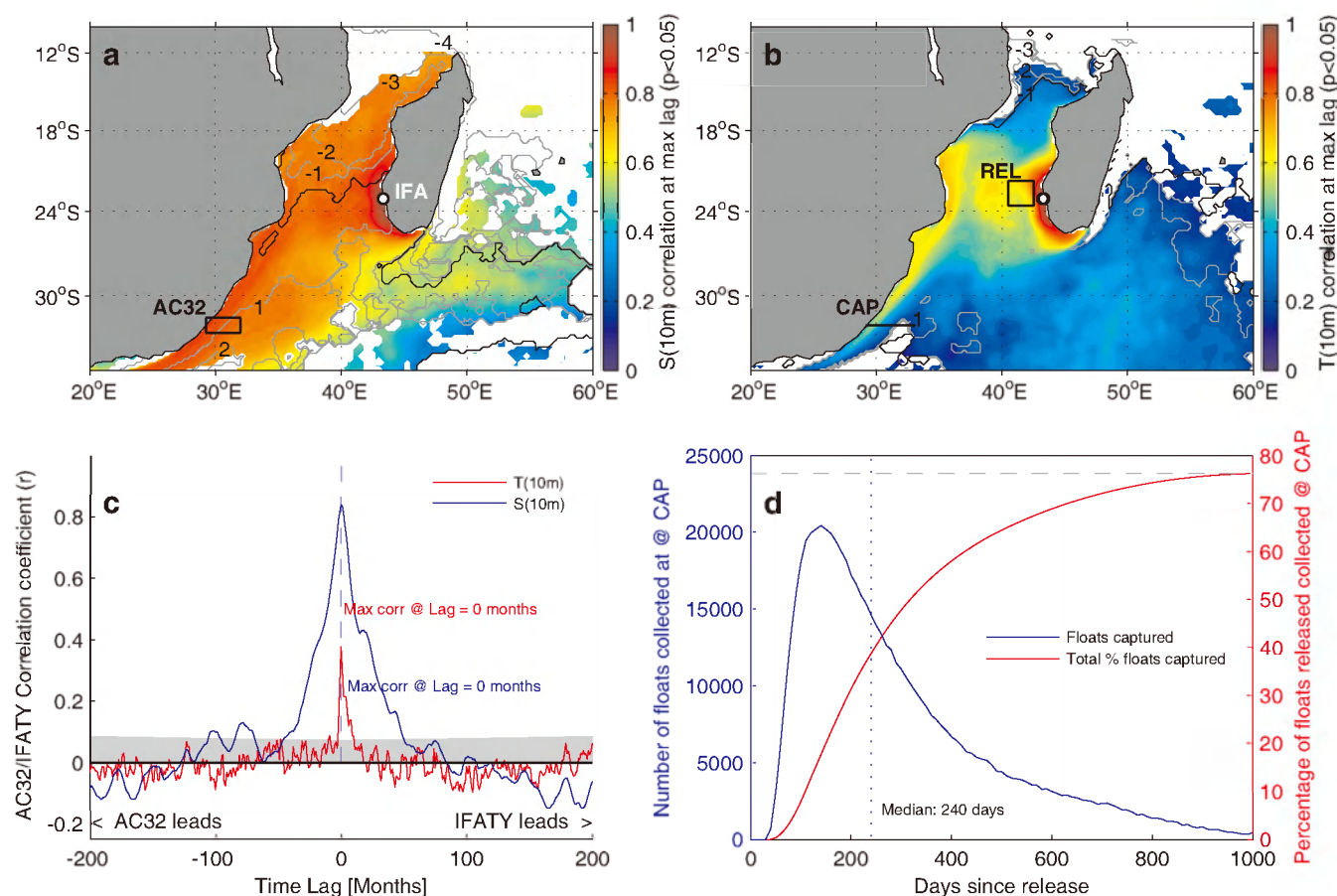


Figure 2 | Connectivity of sea surface temperature (SST), salinity (SSS) and near surface Lagrangian derived advection. (a) Regional correlation with the detrended monthly-mean IFATY surface salinity (SSS) time-series for 1948–2007 (shading, $p < 0.05$). Correlations are plotted at maximum lag, with lag values shown as contours. (b) as in (a) but for SST. (c) lag correlation for SST and SSS between Ifaty and the Agulhas Current at 32°S (represented by the IFA point and AC32 box in panel (a)). (d) Advective connection between Ifaty and the Agulhas Current, as derived from Lagrangian floats released at RE (panel b), and collected at CAP (panel b). Figures produced in MATLAB.

are deployed in the surface waters ($z < 100$ m) at the former location. Figure 2d shows that 76.3% of the particles released reach the AC in 3 years, with a median transit time between the two sites of 240 days. The advective time scale is quite long, whereas the lag between the two SST and SSS signals is near zero (Fig. 2c). This suggests two possibilities: 1) that both sites happen to ‘receive’ the same SST and SSS signal through ocean transport from upstream, or 2) that the signals are driven by large-scale atmospheric processes, influencing both the wider MC area and the AC core region. Nevertheless, our model data confirm the physical link in SST between the MC and the AC core regions and return flow region. The modeling experiments show that the spatial and temporal correlation of SSTs and SSS of the wider Agulhas region is high, including the source areas between the coral sites in the southern MC and the AC core region, for instance in the CAP area at 32°S.

Coral-based SST reconstruction for the southern Mozambique Channel and the Agulhas Current core region. The new SST reconstruction is based on three *Porites* coral oxygen isotope ($\delta^{18}\text{O}$) records at annual resolution from Ifaty and Tulear coral reefs off southwestern Madagascar, 43°E, 23°S, covering the past 334 years (Fig. 3a; Fig. S1). The new coral composite comprises three corals from 1905 to 1994, two from 1881 onwards and a single coral covering 1660 to 1880 (Fig. 3b). The coral proxy data and measurement procedures are described in detail in the Methods. In brief, all proxy records were centered by removing the 1961–1990 mean. A composite annually resolved coral temperature record was

then constructed by (1) converting each $\delta^{18}\text{O}$ record to temperature units, (2) calculating the arithmetic mean of the coral SST records from each site, and (3) averaging the mean SST records from both sites (Fig. S1). For the proxy-temperature conversion, we use the mean of the published $\delta^{18}\text{O}$ -temperature relationship³⁰ ($-0.2\text{‰}/^{\circ}\text{C}$ for $\delta^{18}\text{O}$). This has the advantage that our coral temperature reconstruction does not depend on linear regression with instrumental SST data, which has rather large errors³¹. The composite chronology extends from 1660 to 1994 (Fig. 3).

The composite SST record indicates strong multidecadal variability throughout the 334 years. The composite mirrors the interannual and decadal variability of AC core region SST since 1854 in ERSST, since 1850 in HadSST3 and since 1870 in HadSST1 (Figure 3). The coolest period in SW Madagascar and the AC core region on record pre-1900 is observed between 1675 and 1720 and includes the Late Maunder Minimum (1675–1710), the coolest period during the Little Ice Age. The cool period shows strong interannual variability. The warmest periods on record pre-1900 for both SW Madagascar and the AC core region are observed between 1660–1670, 1770 to 1805, and 1870 to 1900. The warming rate between 1720 and 1800 was rapid at $0.13 \pm 0.02^{\circ}\text{C}/\text{decade}$. The warm period between 1870 to 1900 is also very prominent for both SW Madagascar and the AC core region. This period is punctuated by strong interannual warm anomalies with cooler years in between. Similarly strong interannual variability is also observed for the 1770 to 1805 warm period. SST was lower in the early 20th century and increased markedly after 1970 for both SW Madagascar and the AC core region.

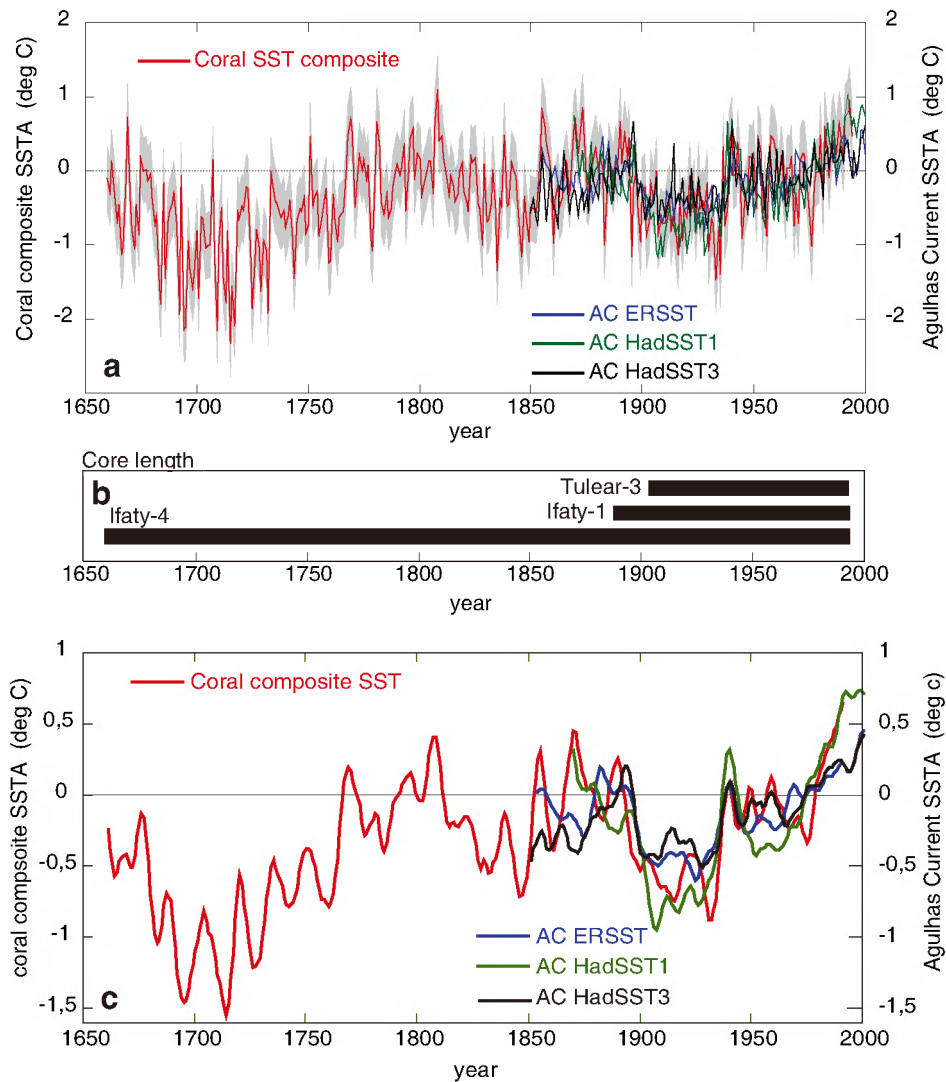


Figure 3 | Sea surface temperature reconstruction for the Agulhas Current region. (a) Coral composite SST anomaly reconstruction for southwestern Madagascar (grey shading shows 2 standard error) compared to Agulhas Current core region data from HadSST1³² (green), ERSSTv3b³⁴ (blue) and HadSST3³³ (black), (b) Time coverage of individual coral core records and (c) Same as (a), yet for filtered data (decadal) with a cutoff of 8 years. All SST anomalies computed relative to the 1961 to 1990 period.

Validation of SST trends in the instrumental and coral SST records.

Absolute warming rates for our coral index and instrumental SST have been estimated using ordinary least squares (OLS) regression, which mainly depends on the $\delta^{18}\text{O}$ -SST conversion. We have estimated the warming rates obtained using published $\delta^{18}\text{O}$ -SST relationships³⁰ with the mean, upper and lower estimates as uncertainty bounds for the regression ($-0.2 \pm 0.02\text{‰/}^\circ\text{C}$). We use the period since 1900 because SST products are less reliable prior to that date.

We found a steady warming in the coral composite SST record since 1900 ($1.07 \pm 0.1^\circ\text{C}$), with most of the increase in the warming rates after 1970 ($1.03 \pm 0.3^\circ\text{C}$). The magnitude of the warming inferred from the corals is $0.12 \pm 0.02^\circ\text{C/decade}$ since 1900 and ranges between 0.13°C and $0.11^\circ\text{C/decade}$ (using the upper and lower limits of $\delta^{18}\text{O}$ -SST relationships). We speculate that much of the observed spread in proxy-SST relationships reflects statistical uncertainties since the error of the OLS regression obtained using the mean slopes equals the spread of the warming rates estimates using the upper and lower limits of proxy-SST relationships. The coral composite SST reconstruction has a higher correlation with instrumental SST for both the Ifaty-Tulear and Agulhas Current core regions than any single coral record (Table 1; Table S1 and S2). The

warming trend after the mid-1970's in the coral composite record agrees substantially better with instrumental SST than the previously published Ifaty-4 coral record alone²⁰.

To validate the trend in our coral composite SST record, we extracted SST records for the Ifaty-Tulear region (centred at 43°E , 23°S) and the AC core region ($26^\circ\text{--}28^\circ\text{E}$, $34^\circ\text{--}36^\circ\text{S}$) from three gridded SST products for the annual average computed from March to February: HadSST1³² from 1870, HadSST3³³ from 1850, and ERSSTv3b (hereafter ERSST³⁴) from 1854 (Fig. 3). All SST products are based on ICOADS data³⁵, but were constructed with different strategies for historical bias correction and gridding. SST data for the Ifaty-Tulear region is based on extremely sparse observations in the ICOADS³⁵ data (Fig. S2). The new $5^\circ \times 5^\circ$ gridded HadSST3 data set is based on a comprehensive reanalysis of the data and metadata in the ICOADS database and is bias-corrected with improved error estimates³³. We identified the gridbox in HadSST3 along the Agulhas Current ($24^\circ\text{--}29^\circ\text{E}$, $31^\circ\text{--}36^\circ\text{S}$) which is the most complete back to 1850 for the greater Agulhas Current region (Fig. 1).

The long-term warming rates indicated by the SST products for the Ifaty-Tulear region since 1900 clearly differ, yet agree on the strong post 1970 warming. The warming rates per decade since



Table 1 | Correlations of detrended, mean annual (March to February) reconstructed SST (If comp = Ifaty/Tulear coral composite SST) with instrumental SST at Ifaty (IF) and for the Agulhas Current (AC) core region. Had1 = HadSST1³², Had3 = HadSST3³³, ERSST³⁴. All correlations significant above the 1% level, despite IF comp with IF Had3 (5%). Correlations computed for maximum number of years in each dataset taking into account the degrees of freedom for each correlation pair. Ifaty HadSST3 suffers from sparse observation pre-1920, while AC HadSST3 is complete to 1850. Correlations computed at <http://climexp.knmi.nl/>⁴²

	IF comp	IF Had1	IF Had3	IF ERSST	AC Had1	AC Had3	AC ERSST
IF comp	1						
IF Had1	0.48	1					
IF Had3	0.34	0.78	1				
IF ERSST	0.37	0.81	0.78	1			
AC Had1	0.57	0.75	0.43	0.64	1		
AC Had3	0.59	0.60	0.31	0.61	0.74	1	
AC ERSST	0.54	0.68	0.49	0.66	0.76	0.70	1

1900 are $0.054 \pm 0.008^{\circ}\text{C}$ (ERSST³⁴), 0.081 ± 0.01 (HadSST1³²) and 0.043 ± 0.01 (HadSST3³³ since 1909). The absolute warming between 1970 to 2005 ranges between $0.39 \pm 0.15^{\circ}\text{C}$ (HadSST3), $0.42 \pm 0.1^{\circ}\text{C}$ (ERSST) and $0.71 \pm 0.12^{\circ}\text{C}$ (HadSST1).

Our coral-based SST reconstruction tracks instrumental AC core region SST since 1854 in ERSST, since 1870 in HadSST1 and since 1850 in HadSST3 (Fig. 3; Tab. 1). We found significant correlations for detrended coral composite SST with AC core region HadSST1 ($r = 0.57$, $P < 0.001$, $DF = 124$), HadSST3 ($r = 0.59$, $p < 0.001$, $DF = 142$) and ERSST ($r = 0.54$, $p < 0.01$, $DF = 140$) for the maximum number of years in each SST dataset (Tab. 1). The correlations were still significant for an early verification period between 1850 to 1910 with AC HadSST3 ($r = 0.62$, $p = 0.0005$, $DF = 59$), although lower with HadSST1 ($r = 0.54$, $p = 0.005$) and ERSST ($r = 0.4$, $p = 0.03$). The correlation between the coral composite and AC core region SST is higher than with Ifaty-Tulear region SST from all SST products (Tab. 1; Tab. S1). This is most probably due to the sparse to non-existent observations for the Ifaty-Tulear region (Fig. S2).

All records, including the coral composite SST, show multidecadal to centennial variability in SST since at least 1870 with two warm periods between 1870 to ~1900 and 1970 to 2005, bracketed by cooler SST in between (Fig. 3). Interannual warm peaks are observed during the 20th century, the most prominent between 1939–1942 and the late 1950's to early 1960's.

Relationships with regional and large-scale temperatures. Our new SST reconstructions also show excellent correlation with an annual mean South African air temperature reconstruction (AT)

from a stalagmite record³⁶ over the entire 334 year period (Fig. 4). The correlation is strongest on decadal time scales applying a Loess filter with a cutoff at 8 years ($r = 0.59$, $p = 0.008$, $N = 308$; Fig. 3c). Both, the coral composite SST and stalagmite AT indicate the period between 1690 to 1740 as the coolest on record. In addition, both records indicate relatively high temperatures during the late 18th and 19th century, a cool period in the early 20th century followed by a warming towards the end of the 20th century.

To assess the correlations of the coral composite with global SST on decadal time scales, we applied a Loess low-pass filter with a cutoff at 8 years. Spatial correlations between coral composite SST and global SST, from HadSST1, revealed statistically significant correlations ($p < 0.05$) on decadal time scales (Fig. 5). The highest correlations are found in the AC region and across the southern Indian Ocean between 20 to 60°S stretching towards the western and southern Australian coast (Fig. 5). Positive correlations also emerge off the eastern coast of South America and the (sub)tropical Atlantic. Other teleconnected regions with positive correlations are the northern Indian Ocean, the western and northeastern Pacific.

We also performed an EOF (Empirical Orthogonal Function) analysis of detrended mean annual HadSST1 in the southern Indian Ocean (10–40°S, 20–130°E) to reveal the dominant SST patterns. EOF1 of HadSST1 showed positive loading across the southern Indian Ocean between South Africa and western Australia. The PC1 time series of this EOF1 pattern resembles the multidecadal SST record for the Agulhas Current region and the coral composite SST (Fig. S3). Our new coral composite SST is strongly related with PC1 showing significant correlations ($p < 0.001$; Suppl. Tables S4 to

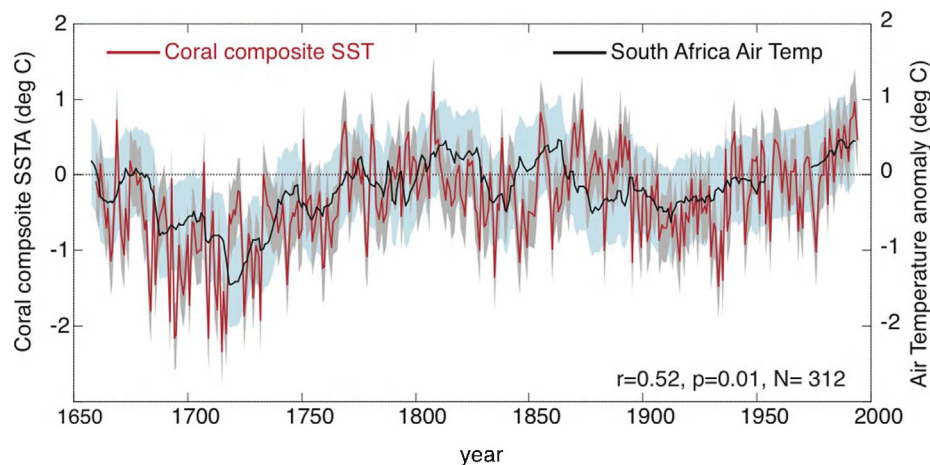


Figure 4 | Reconstructions for sea surface and air temperature for the Agulhas Current and South Africa. Coral composite SST anomaly reconstruction for southwestern Madagascar (grey shading shows 2 standard error) compared to an air temperature reconstruction from stalagmite T7 from Cold Air Cave (24°S, 29°E, 1420 m above sea level) in South Africa³⁶ (blue shading shows 2 standard error). Note the gap in the stalagmite record between 1954 and 1973. Both SST and air temperature anomalies computed relative to the 1961 to 1990 period.

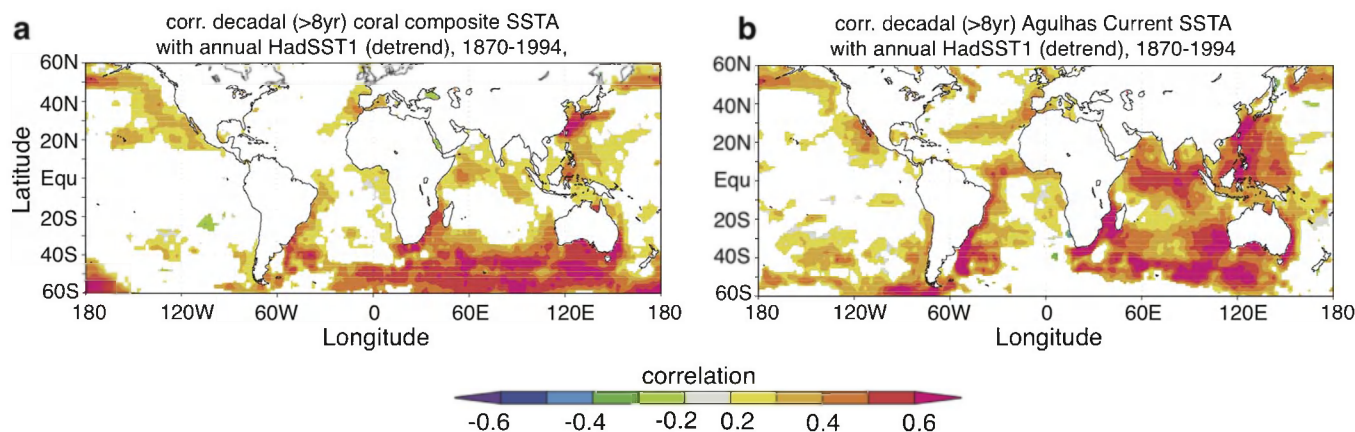


Figure 5 | Global teleconnections of Agulhas Current region sea surface temperature. (a) Spatial correlation of coral-derived SST reconstruction with global HadSST1³² between 1870 to 1994 at decadal time scales (>8 years) and (b) same as (a), yet for Agulhas Current SST from HadSST1³². Correlation with $p < 0.05$ colored. Figure produced at <http://climexp.knmi.nl/>⁴² and used with permission.

S6 and Fig. S3). EOF2 shows a dipole pattern in SST between the southwestern Indian Ocean east of Madagascar and the southeastern Indian Ocean offshore of Indonesia/NW Australia (Fig. S3). This pattern is related to ENSO. PC2 is not correlated with the coral composite when the entire period from 1870 to 1994 is considered. However, after 1950 the correlation is significant ($r = 0.44$, $p < 0.01$, $DF = 40$). This finding is consistent with Zinke et al. (2004)²⁰ who showed evidence for a non-stationary relationship of southern MC SST with ENSO. EOF3 showed a dipole pattern in SST between the tropical and subtropical/mid-latitude Indian Ocean. EOF3 comprises the well-known subtropical dipole modes that can be found across all southern ocean basins, especially in austral summer. The PC3 time series of this EOF3 pattern is positively correlated with our coral composite SST (Suppl. Table S7 and Fig. S3). This finding is consistent with Zinke et al. (2004)²⁰, who showed evidence for a correlation of southern MC SST with the subtropical dipole mode of the southern Indian Ocean.

Discussion

Our new annually resolved coral composite SST reconstruction tracks instrumental AC core region SST since the late 19th century observed in the three SST products: ERSST, HadSST1 and HadSST3. Based on this strong relationship, we are able to resolve historical SST variability and long-term changes in the southern MC and the AC core region back to 1660. We observed strong multidecadal to centennial-scale oscillations in SST over the past 334 years in the coral composite SST and since at least 1850 in three SST datasets. We confirmed the period between 1670 and 1720 as the coolest period on record, which suggests that transport of warm water from the tropical Indian Ocean towards the AC was diminished at this time. We find warm excursions between 1770 and 1800, the late 19th century and post 1976 where warm water transport to the AC was at its peak. The current warming after 1976 to 1994 is not unprecedented since similar warming rates were observed from 1720 to 1800 following peak cooling during the Late Maunder Minimum during the Little Ice Age. Yet, instrumental SST beyond 1994 show that the warming of the past 20 years was exceptional in the context of the past 334 years⁸ (Figs. 1 and 3). However, changes in $\delta^{18}\text{O}$ of seawater through ocean advection and/or precipitation-evaporation changes could have contributed to lower coral $\delta^{18}\text{O}$ and therefore a warm bias during the late 18th century. A previous study coupled (bi)monthly resolved Ifaty $\delta^{18}\text{O}$ and Sr/Ca SST proxies for the a single core (Ifaty-4) and suggested that variations in $\delta^{18}\text{O}$ of seawater might have influenced the SST estimates during the late 18th and 19th centuries²⁰. These periods stand out as particularly warm decades in our new reconstruction. Since our new reconstruction pre-1882 is still

based on the Ifaty-4 record only, a $\delta^{18}\text{O}$ seawater contribution cannot be excluded. Nevertheless, the three instrumental SST datasets agree with the coral composite SST in showing a warm period with strong interannual oscillations pre-1900.

In addition, the recently published air temperature reconstruction for southern Africa from a stalagmite record³⁶ agrees with the coral composite in showing higher temperatures in the region during the late 18th and 19th century (Fig. 4). A rainfall reconstruction for southern Africa³⁷ revealed that the 19th century was wetter than the 20th century which could be partly related to relatively warm SST in the AC region during the early and late 19th century observed in our SST reconstruction. Using observations and AGCM experiments, Reason and Mulenga (1999)³⁸ showed that SSTs in the AC region are related to South African rainfall on interannual and multi-decadal time scales. This adds confidence to the reality of a relatively warm late 19th century in the AC region, only matched and/or exceeded in the period after 1976 (Figs. 1, 3 and 4).

Our reconstruction is in concert with typical spatial teleconnection pattern of the AC region SST with global SST on interannual and decadal time scales. We did not find an ENSO spatial correlation pattern, which agreed with the weak or non-stationary ENSO correlation on seasonal and mean annual time scales with instrumental SST for the AC region²⁰. Yet, we found significant correlations with the western and northeastern Pacific SST. This pattern resembles to some extent the ENSO-like decadal or Pacific Decadal Oscillation pattern in SST²⁷. The strongest relationship was found with the southern Indian Ocean and off the east coast of South America. The strong correlations with the southern Indian Ocean are found along the AC return flow. The teleconnections with the South Atlantic are found along the advective pathways of the Agulhas leakage^{7,39}.

The strongest SST teleconnections across the southern Indian and Atlantic Ocean point to a dominant role of the AC system for SST variability across the subtropical to mid-latitude Indian and Atlantic Ocean (Fig. 5). A recent study of mid-latitude islands across the southern part of all ocean basins also revealed that the Agulhas system is likely a dominant driver of climate variability for the mid- to high latitude Indian Ocean islands⁴⁰. The recent spatial warming trend pattern in the southern Indian Ocean is characterised by two warming centers, one in the southwestern and the other in the southeastern Indian Ocean (Fig. S3). This pattern strongly resembles EOF1 of HadSST1 for the southern Indian Ocean (Fig. S3). PC1 of this EOF1 showed multidecadal SST variability and no linear warming trend (Fig. S3). Thus, the two centers of warming most possibly underwent similar multidecadal SST changes and the recent pattern is part of this natural multidecadal variability. The mechanism



driving this multidecadal variability might be related to large-scale wind forcing across the southern Indian and Atlantic Ocean^{17,41}. Lee et al. (2011)³⁹ showed that the increased heat content across the southern Atlantic since the 1950's was largely related to an increase in inter-ocean heat exchange with the Indian Ocean. The warming in the South Atlantic after 1950 was probably reinforced by a warm Agulhas leakage and its westward and northward transport into the Atlantic. Similar warming of the South Atlantic should have occurred during the late 18th and 19th century according to our AC core region SST reconstruction. This assumption needs to be tested with coupled atmosphere-ocean models.

In conclusion, our new coral composite SST record for the Agulhas Current system showed strong multidecadal SST variability in this globally important ocean current and that the warming over the last three decades is not unprecedented in the context of the multi-centennial record.

Methods

Coral core collection and sampling. Coral cores from massive *Porites* sp. at Ifaty and Tulear reefs were collected in October 1995 during the European Union TESTREFF program from the Ifaty-Ranobé lagoon and the Great Barrier of Tulear (southwest Madagascar²⁰). The Ifaty and Tulear coral reef sites are described in detail in Zinke et al., 2004²⁰ and Bruggeman et al., 2012⁴⁵, respectively. Core Ifaty-4 (4.06 m length), core Ifaty-1 (1.93 m length) and Tulear-3 (1.80 m length) were obtained from a depth of 1.1 m, 1.8 m and 0.6 m below mean tide level. The average growth rate of core Ifaty-4 was 0.99 ± 0.15 cm per year, whereas Ifaty-1 averaged 1.28 ± 0.24 cm and Tulear-3 1.54 ± 0.25 cm per year.

All cores were sectioned to a thickness of 7 mm and slabs were cleaned in 10% hydrogen peroxide for 48 h to remove organic matter at GEOMAR Kiel. Then, slabs were rinsed several times with demineralized water and dried with compressed air. For complete removal of any moisture within the coral skeleton the sample was put into an oven for 24 h at 40°C. The slabs were X-rayed to reveal annual density banding.

A high resolution profile for stable isotope analysis on core Ifaty-4 was drilled using a computer-controlled drilling device along the growth axis as observed in X-ray-radiograph-positive prints²⁰. Subsamples were drilled at a distance of 1 mm for the years 1995–1920 and 2 mm for the older part of the core; the drilling depth was 3 mm using a 0.5 mm dental drill at 1000 rpm. The 1 or 2 mm sample spacing provides approximately monthly or bimonthly resolution, respectively. Cores Ifaty-1 and Tulear-3 were sampled at annual resolution along the major growth axis following the density pattern from summer to summer in any given year established from X-ray-radiograph-positive prints.

Analytical procedures $\delta^{18}\text{O}$. The high-resolution samples of core Ifaty-4 were reacted with 100% H_3PO_4 at 75°C in an automated carbonate reaction device (Kiel Device) connected to a Finnigan MAT 252 mass spectrometer (University Erlangen). Average precision based on duplicate sample analysis and on multiple analysis of NBS 19 is $\pm 0.07\text{‰}$ for $\delta^{18}\text{O}$ (1 σ). The annual samples were reacted with 100% H_3PO_4 at 75°C in an automated carbonate reaction device (Kiel Device) connected to a Finnigan MAT 252 mass spectrometer at the VU University of Amsterdam. Average precision based on duplicate sample analysis and on multiple analysis of NBS 19 is $\pm 0.08\text{‰}$ for $\delta^{18}\text{O}$ (1 σ).

Proxy data treatment. We used the already published, (bi)monthly resolved Ifaty-4 coral $\delta^{18}\text{O}$ time series from 1660 to 1994²⁰. The high resolution of the Ifaty-4 coral $\delta^{18}\text{O}$ enabled us to compute a precise annual chronology averaged between March to February. We used the Ifaty-4 core as our best dated reference time series to ensure that the yearly sampled chronologies of Ifaty-1 and Tulear-3 aligned well. The three proxy records were first centered by removing the 1961–1990 mean. A composite annually resolved coral temperature record was then constructed by (1) converting each proxy record to temperature units, (2) calculating the arithmetic mean of the coral SST records from each site, and (3) averaging the mean records from both sites. For the proxy-temperature conversion we use the mean of the published $\delta^{18}\text{O}$ -temperature relationship ($-0.2 \pm 0.02\text{‰/°C}$ for $\delta^{18}\text{O}$ ³⁰). This resulted in a time series of relative SST changes at annual resolution against the 1961 to 1990 mean.

We estimated the uncertainties of the coral composite SST reconstruction following the method of Nurhati et al. (2011)³¹ for relative SST reconstructions. The errors are displayed in Figure 3 as grey shaded envelopes for each individual year. Uncertainty in the relative annual mean SST reconstruction takes into account errors associated with (i) the analytical precision of the $\delta^{18}\text{O}$ measurements ($\pm 0.4^\circ\text{C}$), and (ii) the calibration slope of the $\delta^{18}\text{O}$ -SST calibration ($\pm 0.1^\circ\text{C}$). Taken together, the annual mean coral $\delta^{18}\text{O}$ -derived SST error is $\pm 0.41^\circ\text{C}$ (1 σ), quadratically combining terms (i)–(ii).

Uncertainty estimates in the relative SST reconstruction trend was estimated taking into account errors associated with (i) the slope error of the SST trend 1900 to 1994 ($\pm 0.16^\circ\text{C}$), (ii) the analytical precision of the $\delta^{18}\text{O}$ measurements ($\pm 0.4^\circ\text{C}$), and (iii) the calibration slope error of the $\delta^{18}\text{O}$ -SST calibration ($\pm 0.1^\circ\text{C}$). Taken together, the twentieth-century coral $\delta^{18}\text{O}$ -derived SST trend error is 0.44°C , quadratically combining terms (i)–(iii).

- Peeters, F. J. C. et al. Vigorous exchange between the Indian and Atlantic oceans at the end of the past five glacial periods. *Nature* **430**, 661–665 (2004).
- Beal, L. M. et al. On the role of the Agulhas system in ocean circulation and climate. *Nature* **472**, 429–436 (2011).
- Biastoch, A., Boening, C. W., Schwarzkopf, U. & Lutjeharms, J. R. E. Increase in Agulhas leakage due to poleward shift of the Southern Hemisphere westerlies. *Nature* **456**, 489–492 (2009).
- Weijer, W., d. Ruijter, W. P. M., Sterl, A. & Drijfhout, S. S. Response of the Atlantic overturning circulation to South Atlantic sources of buoyancy. *Glob. Planet. Change* **34**, 293–311 (2002).
- Biastoch, A., Boening, C. W. & Lutjeharms, J. R. E. Agulhas leakage dynamics affects decadal variability in Atlantic overturning. *Nature* **456**, 489–492 (2008).
- Haarsma, R. J., Campos, E. J. D., Drijfhout, S., Hazeleger, W. & Severijns, C. Impacts of interruption of the Agulhas leakage on the tropical Atlantic in coupled atmosphere-ocean simulations. *Clim. Dynam.* **36**, 989–1003 (2009).
- Rühs, S., Durgadoo, J. V., Behrens, E. & Biastoch, A. Advective time scales and pathways of Agulhas leakage. *Geophys. Res. Lett.* **40**, 3997–4000 (2013).
- Rouault, M., Penven, P. & Pohl, B. Warming in the Agulhas system since the 1980's. *Geophys. Res. Lett.* **36**, L12602 (2009).
- Backeberg, B. C., Penven, P. & Rouault, M. Impact of intensified Indian Ocean winds on mesoscale variability in the Agulhas system. *Nature Climate Change* **2**, 608–612 (2012).
- Jury, M. R., Enfield, D. B. & Melice, J.-L. Tropical monsoons around Africa: Stability of El Niño-Southern Oscillation associations and links with continental climate. *J. Geophys. Res.* **107**, 3151, 15-1–15-17 (2002).
- Lee-Thorp, J. A. et al. (2001). Rapid climate shifts in the southern African interior throughout the mid to late Holocene. *Geophys. Res. Lett.* **28**, 4507–4510.
- Rouault, M. & Lutjeharms, J. R. E. Air-sea exchange over an Agulhas eddy at the subtropical convergence. *Global Atmos. Ocean. Syst.* **7**, 125–150 (2000).
- Reason, C. J. C. Evidence for the influence of the Agulhas current on regional atmospheric circulation patterns. *J. Climate* **14**, 2769–2778 (2001).
- Singleton, A. T. & Reason, C. J. C. A Numerical Model Study of an Intense Cutoff Low Pressure System over South Africa. *Mon. Wea. Reviews* **135**, 1128–1150 (2009).
- Rouault, M., White, S. A., Reason, C. J. C., Lutjeharms, J. R. E. & Jobard, I. 2002: Ocean–Atmosphere Interaction in the Agulhas Current Region and a South African Extreme Weather Event. *Wea. Forecasting* **17**, 655–669.
- Blamey, R. C. & Reason, C. J. C. Numerical simulation of a mesoscale convective system over the east coast of South Africa. *Tellus A* **61**, 17–34 (2009).
- Reason, C. J. C. Multidecadal climate variability in the subtropics/mid-latitudes of the Southern Hemisphere oceans. *Tellus A* **52**, 203–223 (2000).
- Reason, C. J. C. Sensitivity of the southern African circulation to dipole sea-surface temperature patterns in the south Indian Ocean. *Internat. J. Clim.* **22**, 377–393 (2002).
- Fauchereau, N., Trzaska, S., Richard, Y., Roucou, P. & Camberlin, P. Sea-surface temperature co-variability in the southern Atlantic and Indian Oceans and its connections with the atmospheric circulation in the southern hemisphere. *Internat. J. Clim.* **23**, 663–677 (2003).
- Zinke, J., Dullo, W.-C., Heiss, G. A. & Eisenhauer, A. ENSO and Indian Ocean subtropical dipole variability is recorded in a coral record off southwest Madagascar for the period 1659–1995. *Earth Planet. Sci. Lett.* **228**, 177–194 (2004).
- Behera, S. K. & Yamagata, T. Subtropical SST dipole events in the southern Indian Ocean. *Geophys. Res. Lett.* **28**, 327–330 (2001).
- Reason, C. J. C. & Rouault, M. ENSO-like decadal variability and South African rainfall. *Geophys. Res. Lett.* **29**, 10.1029 (2002).
- Hermes, J. C. & Reason, C. J. C. Annual cycle of the South Indian Ocean (Seychelles-Chagos) thermocline ridge in a regional ocean model. *J. Geophys. Res.* **113**, C04035 (2008).
- Fetter, A., Lutjeharms, J. R. E. & Matano, R. P. Atmospheric driving forces for the Agulhas Current in the subtropics. *Geophys. Res. Lett.* **34**, L15605 (2007).
- Lee, T. & McPhaden, M. J. Decadal phase change in large-scale sea level and winds in the Indo-Pacific region at the end of the 20th century. *Geophys. Res. Lett.* **35**, L01605 (2008).
- Nidheesh, A. G., Lengaigne, M., Vialard, J., Unnikrishnan, A. S. & Dayan, H. Decadal and long-term sea level variability in the tropical Indo-Pacific Ocean. *Clim. Dynam.* **41**, 381–402 (2013).
- Crueger, T., Zinke, J. & Pfeiffer, M. Patterns of Pacific decadal variability recorded by Indian Ocean corals. *Int. J. Earth Sci.* **98**, 41–52 (2009).
- McClanahan, T. R., Atweberhan, M., Omukoto, J. & Pearson, L. Recent seawater temperature histories, status, and predictions for Madagascar's coral reefs. *Mar. Ecol. Prog. Ser.* **380**, 117–128 (2008).
- Loveday, B. R., Durgadoo, J. V., Reason, C. J. C., Biastoch, A. & Penven, P. Decoupling of the Agulhas Current from the Agulhas Leakage. *J. Phys. Oceanogr.* (submitted).
- Juillet-Leclerc, A. & Schmidt, G. A calibration of the oxygen isotope paleothermometer of coral aragonite from *Porites*. *Geophys. Res. Lett.* **28**, 4135–4138 (2001).
- Nurhati, I. S., Cobb, K. M. & Lorenzo, E. D. Decadal-Scale SST and Salinity Variations in the Central Tropical Pacific: Signatures of Natural and Anthropogenic Climate Change. *J. Climate* **24**, 3294–3308 (2011).



32. Rayner, N. A. *et al.* Global analyses of sea surface temperature, sea ice, and night marine air temperature since the late nineteenth century. *J. Geophys. Res.* **108**, 4407 (2003).
33. Kennedy, J. J., Rayner, N. A., Smith, R. O., Saunby, M. & Parker, D. E. Reassessing biases and other uncertainties in sea-surface temperature observations since 1850 part 2: biases and homogenisation. *J. Geophys. Res.* **116**, D14104 (2011).
34. Smith, T. M., Reynolds, R. W., Peterson, T. C. & Lawrimore, J. Improvements to NOAA's historical merged land-ocean surface temperature analysis (1880–2006). *J. Climate* **21**, 2283–2296 (2008).
35. Woodruff, S. D. *et al.* ICOADS Release 2.5: Extensions and enhancements to the surface marine meteorological archive. *Int. J. Climatol.* **31**, 951–967 (2011).
36. Sundqvist, H. S. *et al.* Evidence of a large cooling between 1690 and 1740 AD in southern Africa. *Sci. Rep.* **3**, 1767, DOI:10.1038/srep01767 (2013).
37. Neukom, R. *et al.* Multi-proxy summer and winter precipitation reconstruction for southern Africa over the last 200 years. *Clim. Dynam.*, DOI:10.1007/s00382-00013-01886-00386 (2013).
38. Reason, C. J. C. & Mulenga, H. Relationships between South African rainfall and SST anomalies in the Southwest Indian Ocean. *Int. J. Climatol.* **19**, 1651–1673 (1999).
39. Lee, S. K. *et al.* What caused the significant increase in Atlantic Ocean heat content since the mid-20th century? *Geophys. Res. Lett.* **38**, L17607 (2011).
40. Richard, Y. *et al.* Temperature changes in the mid- and high-latitudes of the Southern Hemisphere. *Int. J. Climatol.* **33**, 1948–1963 (2013).
41. Durgadoo, J. V., Loveday, B. R., Reason, C. J. C., Penven, P. & Biastoch, A. Agulhas leakage predominantly responds to the Southern Hemisphere westerlies. *J. Phys. Oceanogr.* **43**, 2113–2131 (2013).
42. van Oldenborgh, G. J. & Burgers, G. Searching for decadal variations in ENSO precipitation teleconnections. *Geophys. Res. Lett.* **32**, L15701 (2005).
43. Bruggemann, H. *et al.* Social-ecological problems forcing unprecedented change on the latitudinal margins of coral reefs: the case of southwest Madagascar. *Ecol. Soc.* **17**, 47 (2012).
44. Carton James, A. & Giese Benjamin, S. A Reanalysis of Ocean Climate Using Simple Ocean Data Assimilation (SODA). *Mon. Wea. Rev.* **136**, 2999–3017 (2008).

Acknowledgments

This work was supported as part of the SINDOCOM grant under the Dutch NWO program 'Climate Variability', grant 854.00034/035. Additional support comes from the NWO ALW project CLIMATCH, grant 820.01.009, and the Western Indian Ocean Marine Science Association through the Marine Science for Management programme under grant MASMA/CC/2010/02. JZ was supported by an Indian Ocean Marine Research Centre UWA/AIMS/CSIRO collaborative assistant professorial fellowship. BL was supported by the European Community's Seventh Framework Programme FP7/2007–2013–Marie-Curie 'GATEWAYS' ITN, grant agreement 238512, and ICE-MASA. Financial support to WCD through the Leibniz Award (DU 129/33) is very much appreciated. Model simulations were performed at DST/CSIR CHPC, Cape Town. We acknowledge support from the SCOR/WCRP/IAPSO working group 136 on the climatic importance of the greater Agulhas system. We thank the VU University Amsterdam (Netherlands) for assistance with stable isotope analysis, especially Suzan Verdegaal. With thank Georg Heiss from the Free University of Berlin and the EU TESTREFF party for sampling the coral cores.

Author contributions

J.Z., B.L. and C.J.C.R. designed the study. J.Z. analysed the coral and instrumental data. B.L. and C.J.C.R. provided and analysed the ocean model data and EOF's. J.Z., B.L. and C.J.C.R. wrote the initial draft, in discussion with C.D. and D.K. All authors helped with the interpretation of the data and writing the manuscript.

Additional information

Supplementary information accompanies this paper at <http://www.nature.com/scientificreports>

Competing financial interests: The authors declare no competing financial interests.

How to cite this article: Zinke, J., Loveday, B.R., Reason, C.J.C., Dullo, W.-C. & Kroon, D. Madagascar corals track sea surface temperature variability in the Agulhas Current core region over the past 334 years. *Sci. Rep.* **4**, 4393; DOI:10.1038/srep04393 (2014).



This work is licensed under a Creative Commons Attribution-NonCommercial-NoDerivs 3.0 Unported license. To view a copy of this license, visit <http://creativecommons.org/licenses/by-nc-nd/3.0>